Published in final edited form as:
Anal Chem. 2012 March 20; 84(6): 2949–2954. doi:10.1021/ac3000368.

Carbon-Ring Microelectrode Arrays for Electrochemical Imaging of Single Cell Exocytosis: Fabrication and Characterization

Yuqing Lin[1], **Raphaël Trouillon**[1], **Maria I. Svensson**[1], **Jacqueline D. Keighron**[2], **Ann-Sofie Cans**[2], and **Andrew G. Ewing**[1,2,*]

[1]Department of Chemistry and Molecular Biology, University of Gothenburg, S-41296, Gothenburg, Sweden

[2]Department of Chemical and Biological Engineering, Chalmers University of Technology, S-41296 Gothenburg, Sweden

Abstract

Fabrication of carbon microelectrode arrays, with up to 15 electrodes in total tips as small as 10 to 50 μm, is presented. The support structures of microelectrodes were obtained by pulling multiple quartz capillaries together to form hollow capillary arrays before carbon deposition. Carbon ring microelectrodes were deposited by pyrolysis of acetylene in the lumen of these quartz capillary arrays. Each carbon deposited array tip was filled with epoxy, followed by beveling of the tip of the array to form a deposited carbon-ring microelectrode array (CRMA). Both the number of the microelectrodes in the array and the tip size are independently tunable. These CRMAs have been characterized using scanning electron microscopy, energy dispersive X-ray spectroscopy, and electrogenerated chemiluminescence. Additionally, the electrochemical properties were investigated with steady-state voltammetry. In order to demonstrate the utility of these fabricated microelectrodes in neurochemistry, CRMAs containing eight microring electrodes were used for electrochemical monitoring of exocytotic events from single PC12 cells. Subcellular temporal heterogeneities in exocytosis (*ie.* cold spots *vs.* hot spots) were successfully detected with the CRMAs.

Keywords

microelectrode arrays; single cell; electrochemical imaging; PC12 cells

INTRODUCTION

A better understanding of the molecular basis of neurotransmitter release at the single cell level is of paramount importance to elucidate the mechanisms of cell-to-cell communication. The key dynamic event in neuronal communication is the release of transmitter molecules through a process called exocytosis. To obtain fast, sensitive, spatially resolved analysis of single cell exocytosis, robust and reliable cellular analysis systems are required. Several techniques, including patch-clamp capacitance detection, optical spectroscopy, and electrochemical sensing with ultra-microelectrodes, have been developed and used to investigate these events.[1] In particular, electrochemical methods, where the released neurotransmitters are oxidized at the surface of a microelectrode, offer the unique advantages of providing quantitative information about the amount of released molecules and precise kinetic characteristics with high sensitivity and sub-millisecond time

*Corresponding Author: andrewe@chalmers.se, fax: +46317722785.

resolution.[2–6] For instance, several reports using amperometry have found significant quantitative and kinetic information, and have proposed various cellular or molecular mechanisms controlling exocytosis.[7–11]

A microelectrode array, possessing all the advantages of a single microelectrode, can significantly improve single cell analysis by providing insights on the spatial variability of biological events. Microelectrode arrays can be divided into two categories, parallel microelectrode arrays, where all the electrodes are connected together and individually addressable microelectrode arrays, where each individual microelectrode is independent from the others and has its own connection to a potentiostat. Compared to the parallel microelectrode arrays, individually addressable microelectrode arrays offer many advantages for biological investigations, in particular high spatial resolution and the possibility of sensing multiple analytes simultaneously in a complex biological sample.

Three main techniques including photolithography, screen-printing, and assembly of electrode materials have been reported and used to fabricate individually addressable microelectrode arrays.[12] Photolithography is widely used as a micro-fabrication technique to create regular metal or carbon electrode arrays.[13–16] Screen-printing is typically used for fabrication of relatively large structures, allowing the production of disposable microelectrodes.[17–20] When electrode arrays are made by assembly of specific electrode materials, manual assembly of the different elements are usually required. Physically assembling the electrode offers the possibility to test a wide range of electrode materials such as gold, platinum, silver, nickel, different carbon surfaces, etc. More importantly, no special laboratory equipment is needed, making these devices widely available and relatively simple to build. Bond and coworkers[21] and Compton and coworkers[22] made individually addressable 10×10 gold electrode microarrays or platinum micro-disk linear arrays by embedding 254-μm-diameter gold or 29-μm-diameter platinum wires into epoxy. Walt and coworkers[23] fabricated ring-shaped gold microelectrode arrays by randomly embedding 25-μm-diameter optical glass fibers coated with gold self-assembled monolayers into epoxy. The idea was then improved upon to fabricate arrays by assembling 11-μm-diameter silica capillaries with inner wall deposited with gold film inside a 2.2-mm-diameter and 2.2-cm-length capillary array.[24] However, creating a perfectly regular and highly dense microelectrode array is still highly challenging because of the physical nature of the assembly process.

Carbon electrodes are widely used in electroanalytical chemistry. They offer a wide potential window and the possibility to control the available surface activity by chemical modification of the functional groups at the carbon/electrode surface or by chemical[25–27] or electrochemical pretreatment.[28–30] Regularly patterned addressable carbon microelectrodes arrays are suitable for acquiring molecular images of small (micrometer to sub-micrometer) areas with high spatial and temporal resolution. These devices can be used to measure the release of electroactive substances across the surface of a single cell, which makes them an excellent tool when searching for spatial resolution in measurements of single cell metabolism, *in vitro* modeling of intercellular communication, or *in vivo* fast scan cyclic voltammetry of release patterns in the living brain.

Few studies have evaluated the reliability and performance of individually addressable carbon microelectrode arrays. In particular, addressing each electrode individually in such small structures can be extremely challenging. The Michael group reported a method to construct two or four individually addressable carbon ultra-microelectrodes (radii~1 μm) in arrays by mounting individual fibers into the separate barrels of four-barreled glass tubing.[31] These electrochemical arrays were used to simultaneously probe dopamine release in the brain at multiple sites. To study, both spatially and temporally, neurotransmitter release from

single pheochromocytoma (PC12) cells, Zhang et al. reported the fabrication and characterization of closely packed carbon fiber disk microelectrode arrays.[32, 33] The carbon micro-disk arrays were made by inserting carbon fibers into each barrel of a multi-barreled glass capillary to create arrays of two, three, and seven electrodes.

In this paper, we report a new and facile method to produce carbon microring electrode arrays. Briefly, these arrays are made by pyrolizing hydrocarbon inside clusters of quartz capillaries. This procedure offers a very flexible fabrication method, without using commercial multi-barreled glass capillaries. The number of electrodes in the array is tunable, and we report arrays featuring from 8 to 15 electrodes in a single tip. Cutting and beveling the array can be used to adjust the tip size from 10 to 50 μm to fit the experimental requirements based on the end application, such as measurements at individual neuronal cells or cell networks. The fabrication method avoids complicated wiring since the deposited carbon in each quartz capillary acts as the electrode as well as the connection. As the electrode barrels are twisted, we developed a procedure involving electrogenerated chemiluminescence (ECL) to spatially identify each electrode in the array. These electrodes have excellent electrochemical properties and high measurement repeatability. The microelectrode arrays were used for multi-site sensing of exocytosis in a single PC12 cell.

EXPERIMENTAL SECTION

Supporting information

Chemicals, scanning electron microscopy and energy dispersive X-ray spectra, electrogenerated chemiluminescence, basic electrochemical parameters, and single cell methods are described in the supporting information.

Fabrication of CRMAs

Fabrication of the multi-barreled capillary arrays—The fused silica capillaries were rinsed with pure water, dried in air and then cut into pieces of approximately 8 cm long (photos showing the fabrication process are shown in Figure S1, Supporting Information). Several 8-cm-long capillaries were initially packed and held together at one end with tape to form multi-barreled capillaries of eight to fifteen barrels. The capillaries were then twisted and bound together on the other end of the array with tape. This multi-barreled capillary was manually pulled into two conical multi-barreled capillaries with a very sharp tip by heating the middle of the multi-barreled capillary with a butane/oxygen torch flame. Finally, the sharp tip of the produced conical multi-barreled capillary was cut off with a scalpel under an optical microscope to remove the heat-soldered part and fabricate a multi-barreled capillary.

Pyrolytic deposition of carbon films—Multibarrel capillaries were supported with a nut and a graphite ferrule to help hold the capillaries in place. Epoxy (5 Minute Epoxy, ITW Performance Polymers and Fluids) was poured into the gap between each capillary and the gap between the graphite ferrule and the multi-barreled capillary to prevent gas leakage during carbon deposition. After curing the epoxy, the multi-barreled capillary was connected to a stainless steel T-joint, where the other two branches were linked to a system providing nitrogen and acetylene separately. Before carbon deposition, a mixed stream of nitrogen (20 psi) and acetylene (6 psi) was fed into the multi-barreled capillary through the two branches to the T-joint for 2 min to drive away the air in the gas line. Finally, carbon films were deposited on the inner surface of the fused silica capillaries by pyrolysis of acetylene, as illustrated in Figure 1A. Carbon deposited on the inside of each capillary, as illustrated in Figure S1, acted as the electrode material as well as the connection wire and eliminated the need for complicated wiring of the independent electrodes, thus allowing fabrication of high density individually addressable microelectrodes. Acetylene (6 psi) was introduced into the

system and was thermally pyrolyzed to pyrolytic carbon by heating the capillary with a butane/oxygen torch flame to produce a black shiny carbon coating onto the inner wall of the multi-barreled capillary.[34–36] After deposition, the flames were slowly removed and the system was left to cool down to room temperature under the nitrogen-acetylene stream. To avoid softening and bending of the small multi-barreled capillary tips, two butane/oxygen torch flames were used together on both sides of the multi-barreled capillary, centered over the tip to obtain symmetrical heating and limiting capillary deformation.

Sealing, electrical contact, and polishing—To seal the capillary and to strengthen the device, the carbon-deposited electrode tips were dipped into freshly prepared epoxy (Epo-Tek, Epoxy Technology) for 20 min and cured in an oven (100 °C) for at least 24 h. The electrode tip was cut and polished at an angle of 45° on a microelectrode beveller (104D fine microgrinder, model BV-10, Sutter Instruments). A copper wire (diameter = 0.1 mm, length = 5 cm) was inserted in each capillary to individually connect each carbon film electrode. The number of microelectrodes included in the array was preselected by the number of quartz capillaries used. In this study, we used eight, ten, twelve and fifteen capillaries to make arrays. The distance between each carbon microring electrode and the total electrode size were important parameters in the response of the CRMAs.[37–40] Due to the conical shape of each pulled capillary and the tapered tip of the whole pulled multi-barreled capillary, the electrode radii and the whole tip size of the array were partially controlled by polishing. As more electrode material was polished away from the tip, the inter-electrode distance and the total tip size were increased achieving CRMAs with tip sizes ranging from 10 μm to 50 μm. Inter-electrode insulation was large enough to prevent current leakage, even when adjacent carbon-deposited microring electrodes were separated by sub-micrometer-thick glass, due to the high electrical resistivity of silica (10^{16} M·m for fused silica at 20°C),[41] thus limiting the probability of cross-talk.

RESULTS AND DISCUSSION

Fabrication and SEM Analysis

Figure 1A details the steps of the microelectrode array fabrication process. The fabrication begins by twisting a bundle of clean capillaries and then manually pulling capillaries into two conical hollow multi-barreled capillaries. Black carbon films are then deposited on the clean fused silica multi-barreled capillary supports by pyrolysis of acetylene. The capillary and the deposited carbon are sealed with epoxy and beveled as described in the Experimental Section. The success rate for the fabrication of eight-electrode CRMAs is around 65%. This was found to decrease as the number of electrodes increases: around 40% of the 16-electrode CRMAs were functional. The sequence of these steps is shown from left to right across Figure 1A for a CRMA with 8 electrodes, ending with a schematic of single cell placement for exocytosis measurements.

Figure 1B shows typical SEM images of CRMAs containing eight, ten, twelve and fifteen microelectrodes. These arrays in Figure 1B are structurally well defined, and the overall diameters of these CRMAs are between 15 and 25 μm, respectively. This diameter can be adjusted during the cutting and beveling process. The carbon-deposited microelectrodes in these arrays are tightly packed together and surrounded by a thin layer of fused silica (~1–2 μm) and an epoxy matrix.

Identifying Individual Electrodes with ECL Measurements

In previous work, carbon microelectrode arrays were composed of individually addressed 2.5 μm radius micro-disks embedded in glass, and the number and the arrangement of the microelectrodes included in the array were preselected and fixed by using different multi-

barreled glass capillaries.[32] Owing to the conical shape and tapered tip of the pulled electrode, the geometric pattern was controlled and the relative position of the different electrodes remained unchanged during fabrication. For the present research, and because of the fabrication procedure of the CRMAs, the capillaries are twisted making it difficult to identify how individual electrodes in the array tip are connected to the electric connections running to the potentiostat. We thus imaged the tip of the CRMAs with ECL to correlate the measured electrochemical signal with electrode position.

ECL at microelectrodes has been the subject of numerous studies,[42–46] and the use of ECL at ultra-microelectrodes as well as at nanometer tips as a light source for scanning optical microscopy has been demonstrated recently.[47, 48] In the present work, spatially resolved ECL images of each microelectrode have been obtained by ECL from $[Ru(bpy)_3]^{2+}$ at the CRMAs positioned above the objective of an optical microscope. ECL images monitored at two different eight-electrode microelectrode arrays are shown in Figure 1C. On the left, the bright white rings indicate where electroactive surfaces are located resulting in ECL. Each electrode has been identified in turn by individual application of potential for ECL detection and these are labeled 1–8 (Center) to indicate each electrode. On the right (Figure 1C), microelectrodes in the array have been sequentially added to the image as the potential is applied. In addition to locating each electrode in the array, these images provide some limited information about the size of and geometry of the electrodes.

Elemental and Ring Thickness Analysis

Figure 2A shows an SEM picture of the cross section of a carbon-deposited microring electrode prepared by pyrolysis and the EDX analysis of three regions of the probe tip. In Figure 2B, the EDX signal at 1.74 keV and 0.52 keV corresponds to the appearance of silicon and oxygen in the light grey outer ring confirming the presence of these elements in the fused quartz capillary which acts as the insulator. The EDX signals at 0.25 keV (attributable to carbon) and at 0.52 keV (attributable to oxygen), shown in Figure 2C result from the epoxy, which is used to fill the hollow carbon-deposited capillary. The EDX signal at 0.25 keV in Figure 2D is consistent with the carbon deposited on the inner wall of capillary and the remaining oxygen signal at 0.52 keV might correspond to some C=O functionalities formed during carbon deposition, some residual epoxy from the beveling, or oxygenation of the carbon surface.

The thickness of the carbon layer inside the capillary can be adjusted with the pyrolysis time. SEM images of the tip of the microelectrodes obtained with different pyrolysis times are displayed in Figure S2 (Supporting Information). The thickness of the carbon layer making up the ring of the microelectrodes as a function of pyrolysis time is shown in Figure 2E. At small pyrolysis time (typically 30 s) the films were ~320 nm and at times longer than 3 min the rings were more than 500 nm thick. We chose 3 min pyrolysis times as the standard for measurements here.

Electrochemical Characterization

Figure 3A shows typical voltammograms of $FcCH_2OH$ at a single ring microelectrode with a total tip diameter of 4 μm. As expected from a microelectrode, these voltammograms are sigmoidal, and the half-wave potential (0.15–0.16 V vs. Ag|AgCl) is similar to that for $FcCH_2OH$ oxidation at a larger carbon electrode.[49, 50] The voltammetric waves appear kinetically quasi-reversible at the ring-shaped carbon deposited microelectrodes (wave slopes approximately 150 mV to 180 mV) as shown in Figure S3 (Supporting Information). In addition, for the carbon-deposited microring-electrode array, near-steady-state cyclic voltammograms are obtained at low scan rates (*i.e.* 20 mV/s) and the limiting currents are mostly scan-rate independent (Figure S3).

The voltammetric response of a carbon-deposited microring electrode at 100 mV/s in 1 mM $FcCH_2OH$ is shown in Figure 3A for 50 continuous scans. The steady-state voltammograms are stable, even after 50 cycles, with only a 1.3 % decrease in diffusion limited current (Figure 3A, inset). Moreover, the steady-state current response decreased by only 5 % after storage at room temperature for one month.

Figure 3B shows the steady-state voltammetric behavior of each of the eight electrodes in a CRMA measured simultaneously at 20 mV/s in 1 mM $FcCH_2OH$. The voltammetric response is well defined and has a sigmoidal shape at this scan rate, consistent with microelectrode theory. The measured I_L at each microelectrode ranges from 123 pA to 300 pA. This is considerably smaller than the theoretically predicted value of 429 pA. This difference in limiting current probably results from the non-uniform thickness of the ring electrodes. Another possibility is that the limiting currents at these microelectrodes are hindered by overlap of the different diffusion fields of these densely packed microelectrodes. This assumption is in good agreement with the experimental data in Figure S4. Figure S4 also shows the overall steady-state voltammetric response of a CRMA containing eight microring electrodes when all the electrodes are connected together (named “total” in the figure). The limiting current of total in Figure S4 is in fact 14 % smaller than the sum of the limiting currents individually measured at the eight microelectrodes (Figure S4, 1 to 8), clearly indicating there is overlap of the depletion layers.

Single Cell Electrochemical Imaging

Arrays of micro or nanometer electrodes can be used to electrochemically map the change in easily oxidized substances released from different single secretory vesicles across the surface of cells. Optical microscopy images in Figure 4A and 4B show a CRMA containing eight microelectrodes with a total tip dimension of ~20 μm placed on a single PC12 cell. A glass micropipette containing high K^+ solution (100 mM) was positioned ~60 μm away to stimulate secretion. Figure 4C displays a 180-s amperometric recording of exocytotic events detected with the eight different microelectrodes of the CRMA at a single PC12 cell. Each current transient corresponds to the electrochemical oxidation of catecholamine (dopamine in these cells) molecules released from a single intracellular vesicle.[2] The half-width ($t_{1/2}$) and the number of molecules released for release events observed at each channel were measured and plotted as histograms (Figure S5 and S6). The averaged values of $t_{1/2}$ and of number of molecules obtained for this set of data are calculated (apart from channel 8 which apparently represents a “cold spot” on the cell with no event recorded over 180 s). These values are otherwise consistent from one channel to another.

To obtain a close inspection of the response from each channel and to check if subcellular heterogeneity can be observed in single-cell exocytosis, electrochemical imaging of a PC12 cell as shown in Figure 4 following potassium stimulation is presented in Figure 5. The number of release events (A and B) and molecules (C and D) are used as the reporter to visualize exocytosis from the single PC12 cell, respectively. In Figure 5A and 5B, the area of the cell membrane under channel 8 obviously shows no event and appears to be a “cold spot”. On the contrary, more events were recorded at channels 2, 5 and 7, thus indicating that these sites are “hot spots”. Thus, it appears that the fabricated ring-shaped array electrode format allows the detection of localized exocytosis at a single cell. In addition, the incidence of concurrent events has also been observed and spatially resolved by our CRMA as demonstrated in Figure S7.

CONCLUSIONS

This paper presents the fabrication and characterizations of carbon-deposited microelectrode arrays. These arrays are formed by pyrolysis of acetylene inside the lumen of pulled quartz

capillaries, making up to 15 electrodes in a tip usually less than 50 μm diameter. The electrodes have been characterization by SEM, EDX analysis, and cyclic voltammetry. Spatially resolved ECL images are shown and allow one to correlate individual microelectrodes in the array tip with the potentiostatic connections. The CRMA has been used to spatially monitor exocytotic release at single cells, and to distinguish subcellular spatial heterogeneity in the exocytosis process.

Supplementary Material

Refer to Web version on PubMed Central for supplementary material.

Acknowledgments

We acknowledge the European Research Council (Advanced Grant), Knut and Alice Wallenberg Foundation, the Swedish Research Council (VR), and the National Institutes of Health for financial support.

References

1. Neher E, Marty A. Proc Natl Acad Sci USA. 1982; 79:6712–6716. [PubMed: 6959149]
2. Wightman RM, Jankowski JA, Kennedy RT, Kawagoe KT, Schroeder TJ, Leszczyszyn DJ, Near JA, Diliberto EJ Jr, Viveros OH. Proc Natl Acad Sci USA. 1991; 88:10754–10758. [PubMed: 1961743]
3. Chen C, Hutchison JE, Postlethwaite TA, Richardson JN, Murray RW. Langmuir. 1994; 10:3332–3337.
4. Wightman RM, Finnegan JM, Pihel KTr. Anal Chem. 1995; 14:154–158.
5. Kennedy RT, Huang L, Aspinwall CA. J Am Chem Soc. 1996; 118:1795–1796.
6. Xin Q, Wightman RM. Anal Chem. 1998; 70:1677–1681. [PubMed: 9599575]
7. Dong Y, Heien ML, Maxson MM, Ewing AG. J Neurochem. 2008; 107:1589–1595. [PubMed: 19094057]
8. Adams KL, Puchades M, Ewing AG. Annu Rev Anal Chem. 2008; 1:329–355.
9. Wang W, Zhang SH, Li LM, Wang ZL, Cheng JK, Huang WH. Anal Bioanal Chem. 2009; 394:17–32. [PubMed: 19274456]
10. Ge S, Koseoglu S, Haynes CL. Anal Bioanal Chem. 2010; 397:3281–3304. [PubMed: 20521141]
11. Lin Y, Trouillon R, Safina G, Ewing AG. Anal Chem. 2011; 83:4369–4392. [PubMed: 21500835]
12. Huang XJ, O'Mahony AM, Compton RG. Small. 2009; 5:776–788. [PubMed: 19340821]
13. Jimbo Y, Robinson HPC. Bioelectrochemistry. 2001; 51:107–115. [PubMed: 10910158]
14. Wang K, Fishman HA, Dai HJ, Harris JS. Nano Lett. 2006; 6:2043–2048. [PubMed: 16968023]
15. Liu X, Baronian KHR, Downard AJ. Anal Chem. 2008; 80:8835–8839. [PubMed: 18947203]
16. Keefer EW, Botterman BR, Romero MI, Rossi AF, Gross GW. Nat Nanotechnol. 2008; 3:434–439. [PubMed: 18654569]
17. Craston DH, Jones CP, Williams DE, Elmurr N. Talanta. 1991; 38:17–26. [PubMed: 18965101]
18. Priano G, Gonzalez G, Guenther M, Battaglini F. Electroanalysis. 2008; 20:91–97.
19. Mann TS, Mikkelsen SR. Anal Chem. 2008; 80:843–848. [PubMed: 18181646]
20. Corgier BP, Marquette CA, Blum LJ. J Am Chem Soc. 2005; 127:18328–18332. [PubMed: 16366588]
21. Lee CY, Tan YJ, Bond AM. Anal Chem. 2008; 80:3873–3881. [PubMed: 18412371]
22. Maisonhaute E, White PC, Compton RG. J Phys Chem B. 2001; 105:12087–12091.
23. Szunerits S, Walt DR. Chem Phys Chem. 2003; 4:186–192. [PubMed: 12619418]
24. Monk DJ, Walt DR. J Am Chem Soc. 2004; 126:11416–11417. [PubMed: 15366869]
25. Hongthani W, Fox NA, Fermín DJ. Langmuir. 2011; 27:5112–5118. [PubMed: 21405066]
26. Wooten M, Gorski W. Anal Chem. 2010; 82:1299–1304. [PubMed: 20088562]

27. Kuznetsova A, Popova I, Yates JT, Bronikowski MJ, Huffman CB, Liu J, Smalley RE, Hwu HH, Chen JGG. J Am Chem Soc. 2001; 123:10699–106704. [PubMed: 11674002]
28. Özcan A, Sahin Y. Electroanalysis. 2009; 21:2363–2370.
29. Su WY, Wang SM, Cheng SH. J Electroanal Chem. 2011; 651:166–172.
30. Lin Y, Liu K, Yu P, Xiang L, Li X, Mao L. Anal Chem. 2007; 79:9577–9583. [PubMed: 17994706]
31. Dressman SF, Peters JL, Michael AC. J Neuronsci Meth. 2002; 119:75–81.
32. Zhang B, Adams KL, Luber SJ, Eves DJ, Heien ML, Ewing AG. Anal Chem. 2008; 80:1394–1400. [PubMed: 18232712]
33. Zhang B, Heien ML, Santillo MF, Mellander L, Ewing AG. Anal Chem. 2011; 83:571–577. [PubMed: 21190375]
34. Blaedel WJ, Mabbott GA. Anal Chem. 1978; 50:933–936.
35. Kim YT, Scarnulis DM, Ewing AG. Anal Chem. 1986; 58:1782–1786.
36. McNally M, Wong DKY. Anal Chem. 2001; 73:4793–4800. [PubMed: 11681453]
37. Sandison ME, Anicet N, Glidle A, Cooper JM. Anal Chem. 2002; 74:5717–5725. [PubMed: 12463354]
38. Lee HJ, Beriet C, Ferrigno R, Girault HH. J Electroanal Chem. 2001; 502:138–145.
39. Beriet C, Ferrigno R, Girault HH. J Electroanal Chem. 2000; 486:56–64.
40. Huang WH, Pang DW, Tong H, Wang ZL, Cheng JK. Anal Chem. 2001; 73:1048–1052. [PubMed: 11289416]
41. Serway, RA.; Beichner, RJ.; Jewett, JW. Physics for Scientists and Engineers. Saunders College Publishing; Orlando: 2004.
42. Amatore C, Fosset B, Maness KM, Wightman RM. Anal Chem. 1993; 65:2311–2316.
43. Maness KM, Terrill RH, Meyer TJ, Murray RW, Wightman RM. J Am Chem Soc. 1996; 118:10609–10616.
44. Wightman RM, Curtis C, Flowers PA, Maus RG, McDonald EM. J Phys Chem B. 1998; 102:9991–9996.
45. Szunerits S, Tam JM, Thouin L, Amatore C, Walt DR. Anal Chem. 2003; 75:4382–4388. [PubMed: 14632040]
46. Fiaccabrino GC, Koudelka-Hep M, Hsueh YT, Collins SD, Smith RL. Anal Chem. 1998; 70:4157–4161. [PubMed: 21651253]
47. Zu YB, Ding ZF, Zhou JF, Lee YM, Bard A. J Anal Chem. 2001; 73:2153–2156.
48. Maus RG, Wightman RM. Anal Chem. 2001; 73:3993–3998. [PubMed: 11534727]
49. Deepa PN, Kanungo M, Claycomb G, Sherwood PMA, Collinson MM. Anal Chem. 2003; 75:5399–5405. [PubMed: 14710818]
50. Collinson MM, Wang H, Makote R, Khramov A. J Electroanal Chem. 2002; 519:65–71.

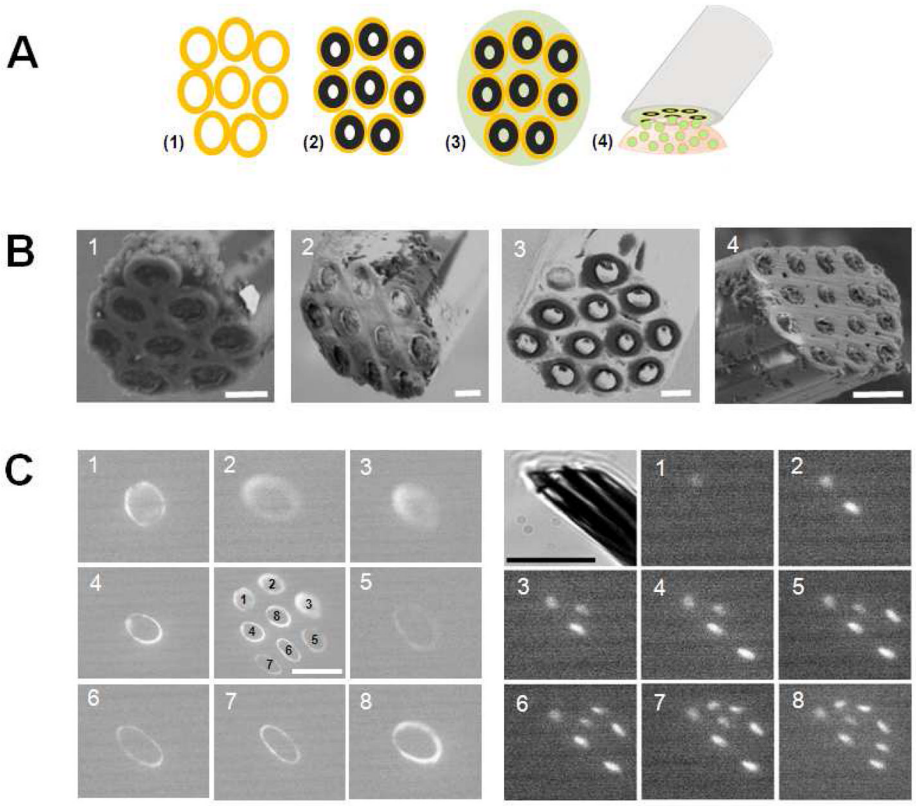

Figure 1.

(A) Schematic of the consecutive steps of the fabrication process of the CRMA, including (1) fused silica multi-barreled capillary, (2) carbon films obtained from pyrolytic deposition on the inner wall of the multi-barreled capillary, (3) the epoxy-sealed carbon deposited microelectrode arrays, and (4) the array positioned on the top of a single cell. (B) Scanning electron microscopy of CRMAs having (1) eight, (2) ten, (3) twelve and (4) fifteen microring electrodes. Scale bars indicate 5 μm. (C) ECL images of two eight electrode CRMAs. Left: the white bright ring indicates identified ECL spots, each frame is an ECL image of an individual microelectrode (labeled from 1 to 8), as shown in the central ECL image of the CRMA. Scale bar in the center indicates 15 μm. Right: white light dots indicate identified ECL spots. Here the ECL images for the individual microelectrodes in the CRMA shown in the top left (optical image of the same array) are connected for ECL beginning with 1 and ending with all 8. Scale bar indicates 20 μm. E = 1.5 V *vs.* Ag|AgCl; exposure time 1 s; 2 mM $Ru(bpy)_3^{2+}$/ 20mM DBAE/ 0.1 M phosphate buffer, pH = 7.5.

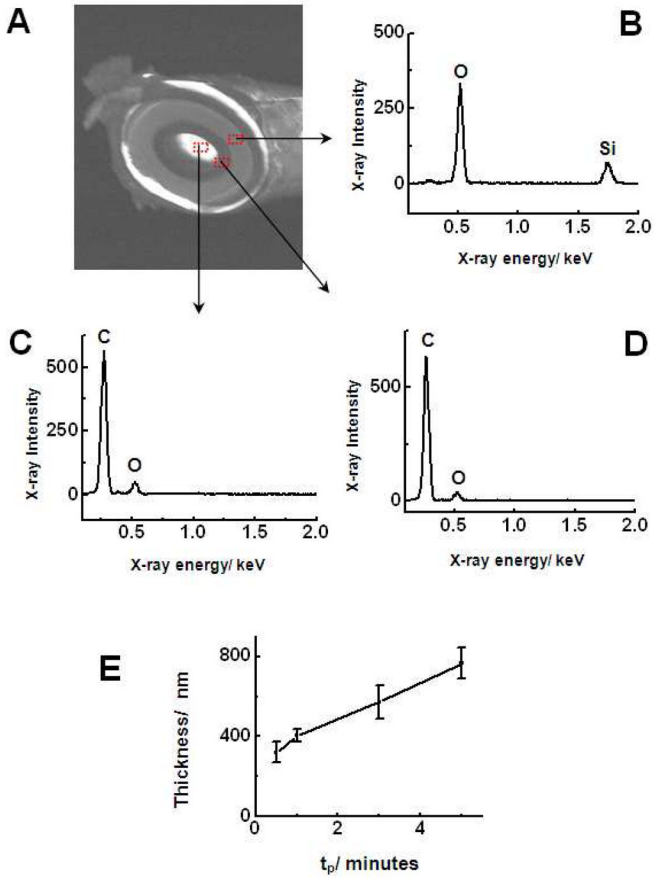

Figure 2.

(A) Scanning electron microscopy of a single carbon microring electrode and EDX spectra performed on (B) the outer ring, (C) the center disk and (D) the middle ring of the device, as indicated by the arrows. (E) Mean thickness of the carbon film, determined by SEM, increasing with longer pyrolysis times (t_p). Each point represents mean ± SD (n = 3 microelectrodes). The center region's bright white color comes from the charging of the insulator. The intercept of this plot is greater than zero suggesting that the pyrolysis and deposition process is very rapid at first and then becomes more constant.

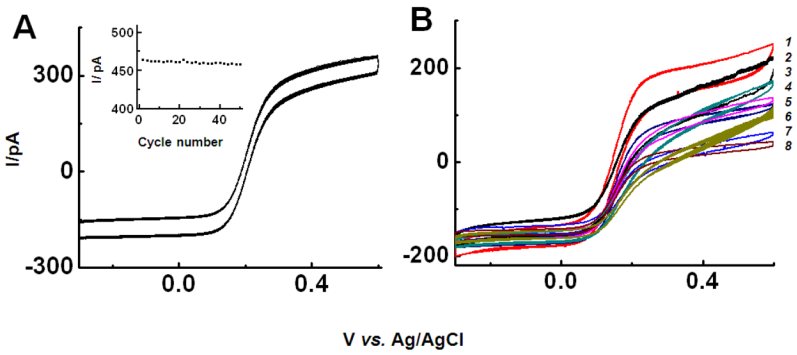

Figure 3.

(A) Continuous steady-state voltammetric response at 100 mV/s for 50 cycles of a carbon-deposited microelectrode in a solution of 1 mM $FcCH_2OH$ in 0.2 M KCl showing overlaid voltammograms and limiting current versus cycle number (inset). (B) Steady-state voltammetric response at 20 mV/s of an eight electrode CRMA in a solution of 1 mM $FcCH_2OH$ in 0.2 M KCl. Voltammetric responses of individual microelectrodes are numbered 1–8.

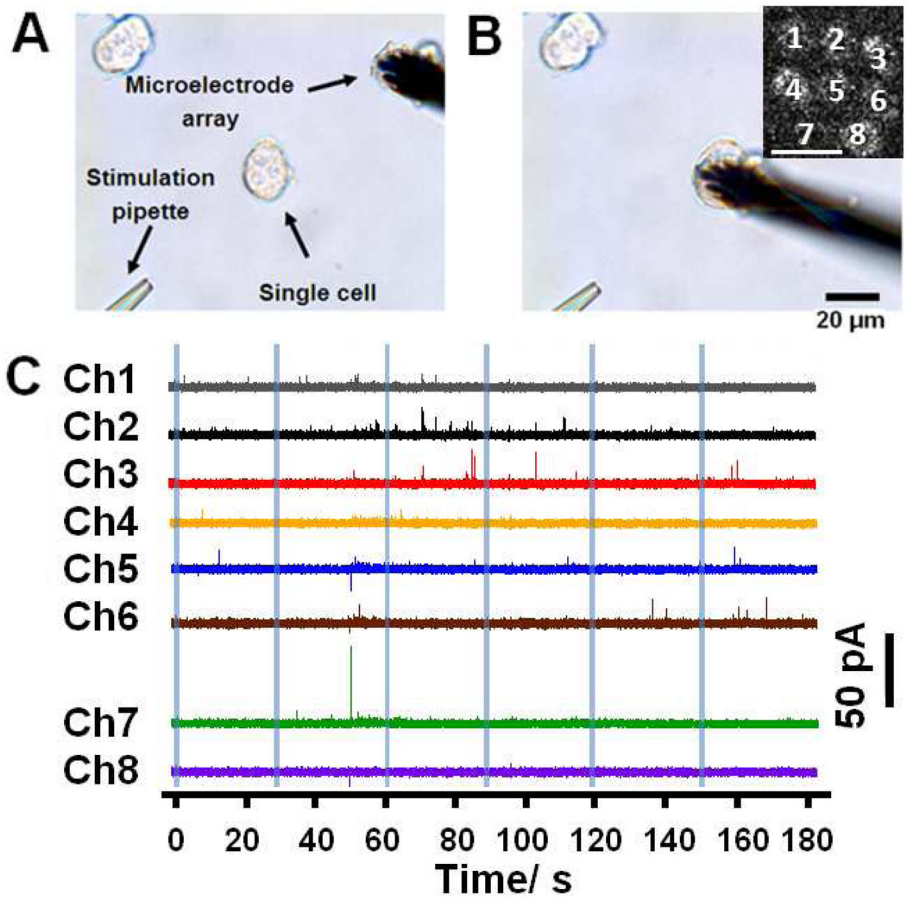

Figure 4.

(A and B) Optical images showing an eight-electrode CRMA before (A) and after (B) positioning on a single PC12 cell. The CRMA, the cell and the stimulation pipette are denoted with arrows. The inserted picture in B is the ECL image of the used CRMA, showing the relative position of each microelectrode in the array (scale bar: 10 μm); (C) Representative amperometric traces of exocytotic release from a PC12 cell recorded using an eight-electrode CRMA. Blue stripes indicate high potassium stimuli (100 mM, 1-s pulse every 30 s).

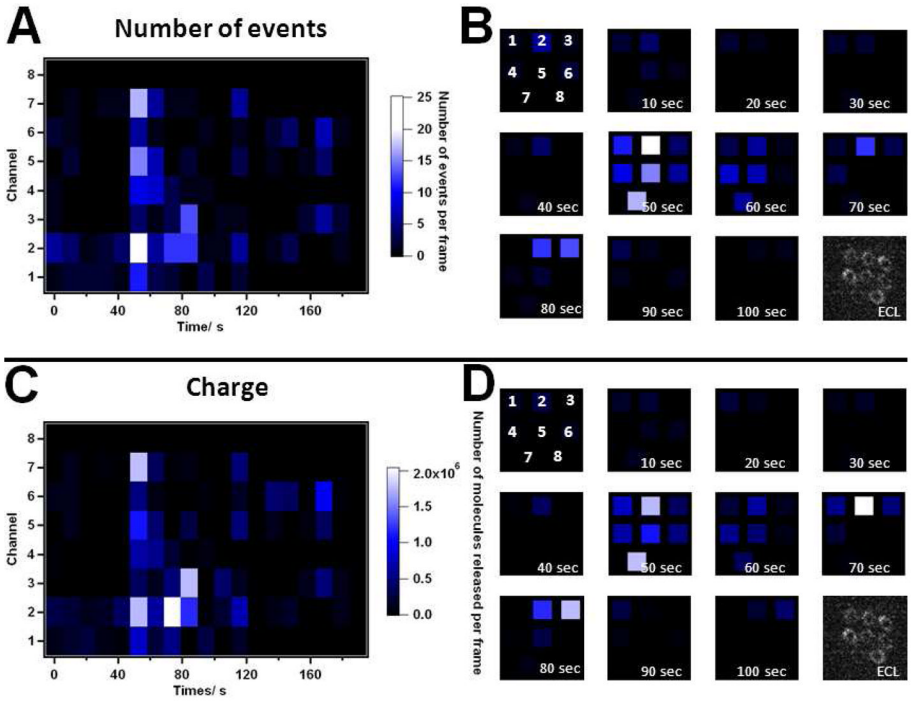

Figure 5.

Electrochemical imaging of the PC12 cell shown in Figure 4 following potassium stimulation. Number of release events (A and B) and charge (C and D) were used as reporters to visualize the PC12 exocytotic activity. Briefly, the data were divided into 10-s frames, and the value of interest (*i.e.* number of events or released charge) was integrated over each frame. (A) Color plots of the number of release events for each electrode in the array integrated over 10-s frames along the horizontal axis. (B) Time variations in event frequency. Each colored square is an independent electrode, and its position on the image has been determined by use of the ECL image shown in the last frame. The color code is the same as (A). (C) Color plots of the released molecules for each electrode in the array integrated over 10 s frames along the horizontal axis. (D) Time variations in released charge. Each colored square is an independent electrode, and its position on the picture has been determined by use of the ECL imaging picture shown on the last frame. The color code is the same as (C).